Inorg. Chem. **2005**, *44*, 9253–9266

Stereochemical Influence of the Ligand on the Structure of Manganese Complexes: Implications for Catalytic Epoxidations

Meenal D. Godbole,[†] Anna C. G. Hotze,[§] Ronald Hage,[#] Allison M. Mills,[‡] Huub Kooijman,[‡] Anthony L. Spek,[‡] and Elisabeth Bouwman*[,†]

Leiden Institute of Chemistry, Gorlaeus Laboratories, Leiden University, P.O. Box 9502, 2300 RA Leiden, The Netherlands, Bijvoet Center for Biomolecular Research, NMR Department, Utrecht University, Unilever R&D Vlaardingen, Olivier van Noortlaan 120, 3133 AT Vlaardingen, The Netherlands, and Bijvoet Center for Biomolecular Research, Crystal and Structural Chemistry, Utrecht University, Padualaan 8, 3584 CH Utrecht, The Netherlands

Received July 22, 2005

Manganese complexes of the ligand HphoxCOOR (R = H or Me) have been synthesized and characterized by X-ray analysis, ESI-MS, ligand-field spectroscopy, electrochemistry, and paramagnetic ^{1}H NMR. The ligands, chirally pure or racemic, influence the structures of the complexes formed. Manganese(III) complexes of the ligand HphoxCOOMe are square-pyramidal or octahedral with two ligands bound in a *trans* fashion in the solid state. The racemic ligand (*RS*-HphoxCOOMe) as well as the enantiopure ligand (*R*-HphoxCOOMe) forms manganese complexes with similar solid-state structures. Ligand-exchange reactions occur in solution giving rise to *meso* complexes as confirmed by ESI-MS and deuteration studies. The manganese(III) complex of *R*-HphoxCOOH is octahedral, with two dianionic ligands bound in a *fac*-cct fashion in a tridentate manner. The manganese(III) complex of *RS*-HphoxCOOH is also octahedral with two dianionic ligands now bound in a *trans* fashion in a didentate manner and with two water molecules occupying axial sites. The paramagnetic ^{1}H NMR spectra of the complexes have been interpreted on the basis of the relaxation times with the help of the inversion-recovery pulse technique. The binding of imidazole with the metal center depends on the chirality of the ligands in the metal complexes of HphoxCOOMe. Imidazole coordination was found to occur with the metal complex that contains two ligands with the same chirality (*R* and *R*) (**R-1**), while no imidazole coordination was found upon reaction with the metal complex that contains two ligands with opposite chirality (*R* and *S*) (**RS-1**). Epoxidation reactions of various alkenes with H_2O_2 as the oxidant reveal that the complexes give turnover numbers in the range of 10–35, the epoxide being the major product. The catalytic activity depends on the additives used, and a clear base effect is observed. The turnover numbers have been found to be higher in the complexes where no binding of *N*-Meim is observed. The latter fact unambiguously shows that imidazole binding is not a prerequisite for higher turnover numbers, in contrast to the Mn–Schiff base catalysts.

Introduction

Single oxygen-transfer reactions are mediated by a variety of metallo-enzymes and biomimetic metal complexes.[1,2] The oxidation of olefins to epoxides is among the key reactions studied in organic chemistry as epoxides can be easily transformed into a large variety of compounds using suitable ring opening reagents. In bulk chemistry, stoichiometric reagents (viz., K_2CrO_7, $KMnO_4$, and derivatives) are usually applied in these reactions.[3−5] However, the use of these reagents has two major disadvantages: it results in high chemical costs and a stoichiometric amount of (often toxic)

* To whom correspondence should be addressed. E-mail: bouwman@chem.leidenuniv.nl.
[†] Leiden Institute of Chemistry, Gorlaeus Laboratories, Leiden University.
[§] Bijvoet Center for Biomolecular Research, NMR Department, Utrecht University.
[#] Unilever R&D Vlaardingen.
[‡] Bijvoet Center for Biomolecular Research, Crystal and Structural Chemistry, Utrecht University.

(1) Costas, M.; Chen, K.; Que, L. *Coord. Chem. Rev.* **2000**, *200*, 517−544.
(2) Lane, B. S.; Burgess, K. *Chem. Rev.* **2003**, *103*, 2457−2473.
(3) Sheldon, R. A. *Top. Curr. Chem.* **1993**, *164*, 21−43.
(4) Sheldon, R. A. *Chemtech* **1991**, *21*, 566−576.
(5) Cornils, B. *Angew. Chem., Int. Ed. Engl.* **1997**, *36*, 2057−2059.

10.1021/ic051223z CCC: $30.25
Published on Web 10/28/2005

inorganic salts as waste is formed.[3,4] Homogeneous catalysis seems to be the perfect alternative, since it ideally involves mild conditions, employs efficient oxidants such as O_2 or H_2O_2, and allows for good tuning of the catalyst, resulting in selective reactions.[6] The progress toward the synthesis of biomimetic model compounds performing oxo transfer has led to a number of synthetically useful catalysts for epoxidation and hydroxylation of organic substrates.[7,8] Since the first reports on Mn(salen)-catalyzed (salen = *N*,*N*′-bis-(salicylidene)-1,2diaminoethane) epoxidations by Srinivasan and Kochi[9] and later on the asymmetric epoxidations independently established by Jacobsen[10] and Katsuki[11] in 1990, the area of Mn−salen-mediated epoxidations has expanded greatly.[12,13] This interest in the Mn(salen) systems is the result of its utility, as well as its intriguing mechanism in terms of catalytic cycle and mode of reaction of active species. For a long time, the complexes suffered from low stability during the highly oxidative conditions during catalytic epoxidation. Further studies on Mn−salen- and Mn−porphyrin-based compounds revealed that the addition of electron-withdrawing substituents on the ligand results in an increased stability and activity of the corresponding Mn compounds in epoxidation reactions.[7,9] A breakthrough was obtained by Ito and Katsuki,[14] when they reported up to 9,200 turnovers and 99% ee (enantiomeric excess) in the epoxidation of 2,2-dimethylchromene derivatives.

One important aspect of the metal-catalyzed epoxidation is the use of various additives that often leads to increased activity. Nitrogen-containing bases such as imidazoles and pyridines are commonly used as additives for effective catalysis with increased selectivity in manganese-catalyzed epoxidations.[15,16] These additives have been proposed to facilitate heterolytic cleavage of the dihydrogen peroxide molecule by coordination to one of the axial sites of the manganese complex for performing efficient oxo transfer. Other additives, such as carboxylic acids, carboxylate, and carbonate salts, have also been reported to cause increased activity.[17−20] The mechanism of action of these additives has been an intriguing topic of study in catalytic epoxidation chemistry.

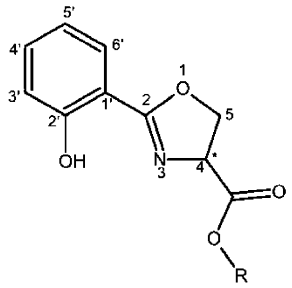

Figure 1. Schematic drawing of the ligand HphoxCOOR (R = CH_3 or H).

Our current research interest is focused on mechanistic studies of olefin epoxidations catalyzed by manganese(III)-phox (Hphox = 2-(2′-hydroxyphenyl)oxazoline) complexes.[21−23] The phox-based ligands have N- and O-donor groups for coordination to the manganese (Figure 1). The stability of the ligands has been proposed to be higher than the salen-type ligands as the oxazoline ring is more stable toward oxidative attack. However, the Mn−phox catalysts developed in our group also appeared to suffer from a lack of stability of the ligand backbone.[22]

The ligands of the type HphoxCOOR contain a stereogenic carbon center (C4); the substituents are at the stereogenic carbon that is closest to the metal center when the ligand coordinates to a metal. These substituents can therefore sterically and chirally affect the approach of molecules toward the metal center and hence induce selectivity. The ligands of the HphoxCOOR type were studied initially by Black and Wade,[24] in relation to the synthesis of mycobactins and their chelating analogues. Mainly, ligands of the *S*-HphoxCOOR type were studied, as the oxazolines present in mycobactins have the *S* configuration at the 4-position. Both the racemic (*RS*) and chiral ligands (*R* or *S*) can be synthesized in a straightforward synthesis from the corresponding serine methyl ester hydrochlorides that are commercially available.

The purpose of this work is to study the coordination behavior of the HphoxCOOR ligands with manganese in detail and examine the catalytic epoxidation activity of the complexes. We have studied the effect of electron-withdrawing substituents (ester and carboxylate groups) as well as the effect of the chirality of the ligand on the catalytic epoxidation activity of the manganese complexes in the presence of various additives. New understanding of the role of imidazole as an additive has been gained; although the addition of imidazole to our catalytic Mn−phoxCOOR system significantly improves the catalytic activity, the activity appeared to be highest in those complexes where imidazole cannot bind to the metal center. Our studies prove that imidazole binding is not necessary for enhanced activity.

(6) Cornils, B.; Herrmann, W. A. *Applied Homogeneous Catalysis with Organometallic Compounds*; VCH: Weinheim, Germany, 1993; p 541.
(7) Gonsalves, A.; Pereira, M. M. *J. Mol. Catal. A* **1996**, *113*, 209−221.
(8) Katsuki, T. *Synlett* **2003**, 281−297.
(9) Srinivasan, K.; Michaud, P.; Kochi, J. K. *J. Am. Chem. Soc.* **1986**, *108*, 2309−2320.
(10) Zhang, W.; Loebach, J. L.; Wilson, S. R.; Jacobsen, E. N. *J. Am. Chem. Soc.* **1990**, *112*, 2801−2803.
(11) Irie, R.; Noda, K.; Ito, Y.; Matsumoto, N.; Katsuki, T. *Tetrahedron Lett.* **1990**, *31*, 7345−7348.
(12) Jacobsen, E. *Asymmetric Catalytic Epoxidation of Unfunctionalized Olefins*; Ojima, I., Ed.; VCH: New York, 1993; pp 159−199.
(13) Katsuki, T. *Coord. Chem. Rev.* **1995**, *140*, 189−214.
(14) Ito, Y. N.; Katsuki, T. *Tetrahedron Lett.* **1998**, *39*, 4325−4328.
(15) Banfi, S.; Maiocchi, A.; Moggi, A.; Montanari, F.; Quici, S. *J. Chem. Soc., Chem. Commun.* **1990**, 1794−1796.
(16) Irie, R.; Ito, Y.; Katsuki, T. *Synlett* **1991**, 265−266.
(17) Pietikainen, P. *Tetrahedron* **1998**, *54*, 4319−4326.
(18) Lane, B. S.; Vogt, M.; DeRose, V. J.; Burgess, K. *J. Am. Chem. Soc.* **2002**, *124*, 11946−11954.
(19) Berkessel, A.; Sklorz, C. A. *Tetrahedron Lett.* **1999**, *40*, 7965−7968.
(20) De Vos, D. E.; Sels, B. F.; Reynaers, M.; Rao, Y. V. S.; Jacobs, P. A. *Tetrahedron Lett.* **1998**, *39*, 3221−3224.
(21) Hoogenraad, M.; Ramkisoensing, K.; Driessen, W. L.; Kooijman, H.; Spek, A. L.; Bouwman, E.; Haasnoot, J. G.; Reedijk, J. *Inorg. Chim. Acta* **2001**, *320*, 117−126.
(22) Hoogenraad, M.; Kooijman, H.; Spek, A. L.; Bouwman, E.; Haasnoot, J. G.; Reedijk, J. *Eur. J. Inorg. Chem.* **2002**, 2897−2903.
(23) Hoogenraad, M.; Ramkisoensing, K.; Gorter, S.; Driessen, W. L.; Bouwman, E.; Haasnoot, J. G.; Reedijk, J.; Mahabiersing, T.; Hartl, F. *Eur. J. Inorg. Chem.* **2002**, 377−387.
(24) Black, D. S. C.; Wade, M. J. *Aust. J. Chem.* **1972**, *25*, 1797−1810.

Experimental Section

Physical Measurements. The ligand-field spectrum in solution was recorded on a Varian Cary 50 Scan UV−vis spectrophotometer. IR spectra were obtained using a Perkin-Elmer FT-IR Paragon 1000 spectrometer equipped with a Golden Gate ATR device. Paramagnetic ^{1}H NMR spectra were recorded using the inversion-recovery pulse sequence with the following typical values: spectral width of 100 ppm, acquisition time of 200 ms, delay time (τ) in the range between 1 μs and 100 ms. The delay between consecutive scans was generally 50 ms. All NMR analyses were performed on a Bruker 300 DPX spectrometer at 300.13 MHz with deuterated methanol or acetonitrile as a reference. Elemental analyses were performed with a Perkin-Elmer series II CHNS/O analyzer 2400. EPR measurements were performed at 77 K using a JEOL Esprit RE−2X spectrometer with a JEOL Esprit 330 ESRE data system. EPR g values were determined relative to DPPH as an external "g marker" ($g = 2.0037$). A Johnson Matthey Alfa products Mk1 magnetic susceptibility balance was used to determine the magnetic moments of the powdered complexes at room temperature. The electrochemistry measurements were performed with an Autolab PGstat10 potentiostat controlled by GPES4 software. A three electrode system containing a glassy carbon (GC) working electrode, a platinum (Pt) auxiliary electrode, and an Ag/AgCl reference electrode was used. The experiments were usually done in a solvent containing acetonitrile/MeOH or acetonitrile/EtOH (20:80 v/v) mixture under an argon atmosphere with tetrabutylammonium hexafluorophosphate as the supporting electrolyte. Under the present experimental conditions, the one-electron oxidation of ferrocene occurs at $E° = +0.40$ V with a peak-to-peak separation of 95 mV. Electrospray mass spectra were recorded on a Thermo Finnigan AQA apparatus. A Varian Star 3400CX gas chromatograph with a J&W Scientific/Fisons DB-1701 (14% cyanopropylphenyl-methylpolysiloxane) column was used for the analysis of the oxidation experiments. Conductivity measurements were performed using a Philips PW9526 digital conductivity meter and a PW9552/60 measuring cell with 1 mM solutions of the complexes in acetonitrile, methanol, or both.

Syntheses. ***Caution:*** *Perchlorate salts are potentially explosive and should be handled with appropriate care. Mixtures of dihydrogen peroxide (35%) and acetone can give an acetone peroxide adduct which is explosive.* Under the given conditions, however, the probability for the formation of the latter is rather low. The following abbreviations are used throughout the text: HphoxCOOMe = methyl 2-(2′-hydroxyphenyl)-oxazoline-4-carboxylate and HphoxCOOH = 2-(2′-hydroxyphenyl)-oxazoline-4-carboxylic acid. All reagents and solvents were used as received with no attempt to remove water or molecular oxygen. Enantiopure (*R* or *S*) or racemic (*RS*) serine methyl ester hydrochloride and serine were ordered from Acros and were used as received. The ligands, methyl salicylimidate, HphoxCOOMe, and HphoxCOOH, were synthesized using the published procedure.[24]

***S*-serine Methyl-d^3 Ester Hydrochloride.** Thionyl chloride (0.5 mL, 6.855 mmol) was added drop-by-drop to a solution of 1 g (1.90 mmol) of *S*-serine in 3 mL of CD_3OD at 0 °C. The solution was allowed to reach room temperature and was stirred for 16 h. On the next day, water was added slowly to the reaction mixture. The solution was then filtered and evaporated to dryness under vacuum. The remaining solid was dissolved in methanol; the solution was dried over $MgSO_4$, filtered, and evaporated to dryness under high vacuum. The faint yellow solid was used without further purification. Yield: 1.9 g (89%). ^{1}H NMR (300 MHz, CD_3OD): δ 3.98 (dd, 2H, CH_2), 4.14 (t, 1H, C*H*). ESI-MS: *m*/*z* 123.02 (100) $[(C_4H_6D_3NO_3) + H^+]^+$.

***S*-HphoxCOOCD$_3$.** The ligand was synthesized in a manner similar to that of the undeuterated ligand using the procedure of Black and Wade.[24] *S*-serine methyl-d^3 ester hydrochloride (0.120 g, 0.76 mmol) was dissolved in 10 mL of deuterated methanol (CD_3OD); then, 0.115 g (0.76 mmol) of methyl salicylimidate was added to the solution. The solution was refluxed for 12 h and stirred at room temperature for 48 h. For workup, the reaction mixture was evaporated to dryness on a rotary evaporator, and the solid was redissolved in dichloromethane. The dichloromethane solution was washed two times with water, and the water extracts were discarded. The dichloromethane extract was dried over $MgSO_4$, filtered, and evaporated to dryness to yield a pinkish-brown oil. Yield: 0.085 g (50%). ^{1}H NMR (300 MHz, $CDCl_3$): δ 7.81 (d, 1H, H6′), 7.64 (t, 1H, H4′), 7.34 (d, 1H, H3′), 6.99 (t, 1H, H5′), 4.93 (dd, 1H, H4a), 4.64 (dt, 2H, H5a and H5b), 2.74 (broad, OH). ESI-MS: *m*/*z* 225.02 (100) $[(S\text{-HphoxCOOCD}_3 + H^+)]^+$.

[Mn(*R*-phoxCOOMe)$_2$Br] (R-1): A solution of 0.5 g (2.26 mmol) of *R*-HphoxCOOMe in 5 mL of MeOH was added to a solution of 0.324 g (1.13 mmol) of manganese(II) bromide in 5 mL of MeOH. The resulting green solution was warmed to 50 °C and stirred for 30 min. The solution was filtered, and crystals were grown in a few days by layering the MeOH solution with diethyl ether. The product was collected by filtration, washed with MeOH and diethyl ether, and dried in air. Yield: 76% (0.68 g). UV−vis (CH_3CN) λ_{max} (ϵ): 434 (1120), 597 nm (417 M^{-1} cm^{-1}). IR (diamond): 2958(w), 1748(vs), 1607(vs), 1585(vs), 1545(s), 1470(s), 1432(s), 1404(s), 1327(s), 1241(vs), 1206(s), 1152(s), 1093(vs), 1026(s), 963(m), 939(w), 862(vs), 757(vs), 704(m), 674(m), 623(m), 573(m), 433(m), 363(m), 310(m) cm^{-1}. Anal. Calcd for **R-1** (fw = 575.25): C, 45.93; H, 3.5; N, 4.87. Found: C, 45.82; H, 3.45; N, 4.97. ESI-MS: *m*/*z* 495.1 (100) $[Mn(phoxCOOMe)_2]^+$, 553.12 (40) $[Mn(phoxCOOMe)_2(acetone)]^+$, 1069.20 (>1) $[Mn^{III}(phoxCOOMe)_2\text{-}Br\text{-}Mn^{III}(phoxCOOMe)_2]^+$.

[Mn(*R*-phoxCOOMe)$_2$Br][Mn(*S*-phoxCOOMe)$_2$Br] (RS-1): A solution of 0.51 g (2.3 mmol) of *RS*-HphoxCOOMe in 5 mL of MeOH was added to a solution of 0.331 g (1.15 mmol) of manganese(II) bromide in 5 mL of MeOH. The resulting green solution was warmed to 50 °C and stirred for 30 min. The solution was filtered, and crystals were grown in a few days by layering the MeOH solution with diethyl ether. The product was collected by filtration, washed with MeOH and diethyl ether, and dried in air. Yield: 67% (0.60 g). UV−vis (CH_3CN) λ_{max} (ϵ): 423 (905), 479 (208), 597 nm (158 M^{-1} cm^{-1}). IR (diamond): 2958(w), 1748(vs), 1607(vs), 1585(vs), 1545(s), 1470(s), 1432(s), 1404(s), 1327(s), 1241(vs), 1206(s), 1152(s), 1093(vs), 1026(s), 963(m), 939(w), 862(vs), 757(vs), 704(m), 674(m), 623(m), 573(m), 433(m), 363(m), 310(m) cm^{-1}. Anal. Calcd for **RS-1** (fw = 575.25): C, 45.93; H, 3.5; N, 4.87. Found: C, 45.85; H, 3.41; N, 5.05. ESI-MS: *m*/*z* 495.1 (100) $[Mn(phoxCOOMe)_2]^+$, 553.18 (40) $[Mn(phoxCOOMe)_2(acetone)]^+$, 1069.12 (<1) $[Mn^{III}{}_2(phoxCOOMe)_4Br]^+$.

[Mn(*R*-phoxCOOMe)$_2$(C$_2$H$_5$OH)(ClO$_4$)] (R-2): A solution of 0.5 g (2.26 mmol) of *R*-HphoxCOOMe was prepared in 10 mL of EtOH; 0.409 g (1.13 mmol) of manganese(II) perchlorate was added to the above solution, and it was warmed to 50 °C for 30 min. The solution slowly turned green. The reaction mixture was then filtered, and the filtrate was layered with diethyl ether to give X-ray quality, dark green crystals of the product, which were collected by filtration, washed with EtOH and diethyl ether, and dried in air. Yield: 56% (0.6 g). UV−vis (CH_3CN) λ_{max} (ϵ): 426 (1120), 603 nm (295 M^{-1} cm^{-1}). IR (diamond): 3551(m), 3480(m), 3005(w), 2954(w), 1740(s), 1607(vs), 1586(vs), 1546(s), 1479(s), 1471(s), 1444(s), 1406(s), 1325(s), 1243(vs), 1220(s), 1161(s), 1088(vs), 961(s), 936(w), 858(vs), 753(vs), 706(m), 677(m), 623(m), 572(m), 436(m), 368-

Table 1. Crystallographic Data for **R-1**, **R-2**, **RS-1**, **R-4**, and **RS-5**

	R-1	RS-1	R-2	R-4	RS-5
formula	$C_{22}H_{20}BrMnN_2O_8$	$C_{22}H_{20}BrMnN_2O_8$	$C_{24}H_{26}ClMnN_2O_{13}$	$C_{20}H_{14}MnN_2O_8,C_4H_{12}N$	$C_{20}H_{18}MnN_2O_{10},C_6H_{16}N$
fw (g/mol)	575.24	575.24	640.86	539.42	603.50
a (Å)	10.7855(1)	12.057(2)	11.4525(2)	11.2381(10)	6.3628(2)
b (Å)	9.6873(1)	12.321(2)	8.9955(1)	17.736(2)	12.0069(3)
c (Å)	11.8322(2)	15.871(2)	13.2330(3)	24.809(3)	18.6764(4
β (deg)	109.4170(10)	107.89(2)	91.6743(7)	-	108.2740(10)
V (Å^3)	1165.94(3)	2243.7(6)	1362.69(4)	4944.9(9)	1354.87(6)
Z	2	4	2	8	2
space group	$P2_1$ (No. 4)	*C*2/*c* (No. 15)	$P2_1$ (No. 4)	$P2_12_12_1$ (No. 19)	$P2_1/c$ (No. 14)
cryst syst	monoclinic	monoclinic	monoclinic	orthorhombic	monoclinic
ρ_{calcd} (g/cm^3)	1.6385(1)	1.7029(5)	1.5619(1)	1.4490(3)	1.4793(1)
T (K)	150	150	150	150	150
μ(Mo Kα) (mm^{-1})	2.329	2.422	0.653	0.587	0.550
total reflns	19150	27679	18563	50739	16781
unique reflns	5227	2581	6154	11280	3063
params	319	155	388	665	179
Flack *x*	-0.004(6)	-	0.000(14)	0.005(11)	−
R, wR2	0.0307, 0.0728	0.0274, 0.0781	0.0410, 0.0815	0.0392, 0.0917	0.0456, 0.1237
S	1.05	1.08	1.00	1.03	1.03

(m), 309(m) cm^{-1}. Anal. Calcd for [**R-2** − 0.5EtOH] (fw = 617.83): C, 44.71; H, 3.75; N, 4.53. Found: C, 44.20; H, 3.64; N, 4.57. ESI-MS: *m*/*z* 495.16 (100) [Mn(phoxCOOMe)$_2$]$^+$, 553.13 (20) [Mn(phoxCOOMe)$_2$(acetone)]$^+$, 1089.07 (1) [Mn$^{III}_2$(phoxCOOMe)$_4$(ClO$_4$)]$^+$.

[Mn(*R*-phoxCOOMe)$_2$(H$_2$O)$_2$][Mn(*S*-phoxCOOMe)$_2$(H$_2$O)$_2$](ClO$_4$)$_2$ (RS-3). A solution of 0.2 g (0.904 mmol) of *RS*-HphoxCOOMe in 5 mL of EtOH was added to a solution of 0.163 g (0.45 mmol) manganese(II) perchlorate in 5 mL of EtOH. The resulting green solution was warmed to 50 °C and stirred for 30 min. The solution was filtered, and slow evaporation of the mother liquor gave dark green crystals. Yield: 49% (0.15 g). UV−vis (CH$_3$CN) λ_{max} (ϵ): 428 (950), 488 (324), 605 nm (271 M^{-1} cm^{-1}). IR (diamond): 2958(w), 1748(vs), 1607(vs), 1585(vs), 1545(s), 1470(s), 1432(s), 1404(s), 1327(s), 1241(vs), 1206(s), 1152(s), 1093(vs), 1026(s), 963(m), 939(w), 862(vs), 757(vs), 704(m), 674(m), 623(m), 573(m), 433(m), 363(m), 310(m) cm^{-1}. Anal. Calcd for **RS-3** (fw = 630.82): C, 41.89; H, 3.83; N, 4.44. Found: C, 42.08; H, 3.99; N, 4.73. ESI-MS: *m*/*z* 495.12 (100) [Mn(phoxCOOMe)$_2$]$^+$, 553.09 (20) [Mn(phoxCOOMe)$_2$(acetone)]$^+$, 1089.01 (1) [Mn$^{III}_2$(phoxCOOMe)$_4$(ClO$_4$)]$^+$.

(H$_2$NEt$_2$) *fac*-cct-[Mn(*R*-phoxCOO)$_2$] (R-4). A solution of 0.3 g (1.44 mmol) of *R*-HphoxCOOH was prepared in MeOH; 0.18 g (0.72 mmol) of solid manganese(II) chloride was added to the solution, after which 1 mL of triethylamine was added. The solution turned green slowly and was warmed to 50 °C for 2 h. The solution was then filtered, and the filtrate was layered with diethyl ether to give X-ray quality, dark green crystals of the product, which were collected by filtration, washed with MeOH and diethyl ether, and dried in air. Yield: 55% (0.213 g). UV−vis (CH$_3$CN) λ_{max} (ϵ): 355(2250), 438 (360), 595 nm (186 M^{-1} cm^{-1}). IR (diamond): 3008(m), 1608(vs), 1584(vs), 1547(s), 1476(s), 1443(s), 1404(s), 1323(s), 1245(vs), 1157(s), 1088(vs), 861(s), 752(vs), 668(m), 575(m), cm^{-1}. Anal. Calcd for [**R-4**·3H$_2$O] (fw = 593.46): C, 48.57; H, 5.43; N, 7.08. Found: C, 48.45; H, 5.63; N, 7.22. ESI-MS: *m*/*z* positive mode 467.10 (100) [Mn(phoxCOO)$_2$ + 2H$^+$]$^+$, negative mode 465.00 (100) [Mn(phoxCOO)$_2$]$^-$.

(HNEt$_3$) *trans*-[Mn(*R*-phoxCOO)(*S*-phoxCOO)(H$_2$O)$_2$] (RS-5). A solution of 0.3 g (1.44 mmol) of *RS*-HphoxCOOH was prepared in 10 mL of acetonitrile/MeOH (1:1); 0.177 g of manganese(II) perchlorate was added to the solution, followed by 0.5 mL of triethylamine. The solution turned green and was warmed to 50 °C for 2 h. The solution was then filtered, and the filtrate was layered with diethyl ether to give X-ray quality, dark green crystals of the product, which were collected by filtration, washed with EtOH and diethyl ether, and dried in air. Yield: 37% (0.160 g). UV−vis (CH$_3$CN) λ_{max} (ϵ): 348 (1520), 444 (260), 601 nm (177 M^{-1} cm^{-1}). IR (diamond): 2978(m), 1615(vs), 1584(vs), 1540(s), 1475(s), 1441(s), 1397 (s), 1325(s), 1245(vs), 1150(s), 1140(s), 1082(vs), 1032(m), 958 (w), 862(vs), 761(vs), 718(m), 676(m), 572(m), 435 (m), 353(m) cm^{-1}. Anal. Calcd for [**RS-5**·2H$_2$O] (fw = 603.5): C, 51.75; H, 5.68; N, 6.96. Found: C, 51.73; H, 5.87; N, 7.12. ESI-MS: *m*/*z* positive mode 467.08 (100) [Mn(phoxCOO)$_2$ + 2H$^+$]$^+$, 525.12 (70) [Mn(phoxCOO)$_2$(acetone) + 2H$^+$]$^+$, negative mode 464.97 (100) [Mn(phoxCOO)$_2$]$^-$.

Epoxidations. General. The alkenes and oxidants were ordered from Acros or Sigma-Aldrich and were used as received without further purification. All reactions were performed in 20 mL vials in air. The catalytic reactions have mainly been carried out in a mixture of methanol/acetone (80:20 v/v), usually with the catalyst to substrate-to-oxidant ratio being 1:100:800. The solid catalyst (10 μmol) was dissolved in 10 mL of the acetone/MeOH (80:20 v/v) mixture with stirring at 0 °C. One millimole of the substrate and 100 μmol of the additive were added to the resulting green solution, followed by a slow drop-by-drop addition of 8 mmol (0.7 mL) of dihydrogen peroxide (35%). A 100 μL sample of the reaction mixture was taken at 3 and 5 h, diluted with acetone to 1 mL, and analyzed by GC using chlorobenzene or decane as the internal standard. The calculated turnovers numbers given are the total turnover numbers per manganese ion after the indicated period of time. All reactions were performed at least in duplicate.

X-ray Crystal Structure Analyses. Pertinent data for the structure determinations are given in Table 1. Data were collected at 150 K on a Nonius KappaCCD diffractometer on rotating anode (graphite-monochromated Mo Kα radiation, λ = 0.71073 Å). The unit-cell parameters were checked for the presence of higher-lattice symmetry.[25] The intensity data for **R-1** and **RS-1** were corrected for absorption using PLATON/DELABS[26] (correction range 0.547−0.867) and PLATON/MULABS (correction range 0.522−0.619), respectively. The structures were solved with direct methods (using SHELXS86[27] for compound **RS-1** and SHELXS97[28] for compounds **R-1** and **RS-5**) or automated Patterson and subsequent difference

(25) Spek, A. L. *J. Appl. Crystallogr.* **1988**, *21*, 578−579.
(26) Spek, A. L. *J. Appl. Crystallogr.* **2003**, *36*, 7−13.
(27) Sheldrick, G. M. *SHELXS-86: Program for X-ray Structure Determination*; University of Göttingen: Göttingen, Germany, 1986.
(28) Sheldrick, G. M. *SHELXS-97: Program for Crystal Structure Determination*; University of Göttingen: Göttingen, Germany, 1997.

Table 2. Selected Bond Distances (Å) and Angles (deg) for Complexes **R-1**, **R-2**, and **RS-1**

R-1		**RS-1**[a]		**R-2**	
Mn1−Br1A[b]	2.5708(5)	Mn1−Br1	2.5550(6)	Mn1−O2	2.374(2)
Mn1−O17	1.858(2)	Mn1−O17	1.8543(13)	Mn1−O6A[c]	2.247(4)
Mn1−N23	1.988(2)	Mn1−N23	1.9777(16)	Mn1−O17	1.8525(18)
Mn1−N43	1.995(2)			Mn1−N23	1.978(2)
Mn1−O37	1.8590(19)			Mn1−N43	1.992(2)
				Mn1−O37	1.8538(19)
Br1A−Mn1−O17	100.36(6)	Br1−Mn1−O17	97.22(5)	O2−Mn1−O6A	175.12(12)
Br1A−Mn1−O37	92.19(6)	Br1−Mn1−N23	98.51(5)	O2−Mn1−O17	88.68(9)
Br1A−Mn1−N23	97.34(6)	O17−Mn1−N23	88.25(6)	O2−Mn1−O37	90.14(9)
Br1A−Mn1−N43	99.00(6)	O17−Mn1−O17a	165.56(7)	O2− Mn1−N23	88.55(9)
O17−Mn1−O37	167.45(9)	O17−Mn1−N23a	89.62(6)	O2−Mn1−N43	87.96(9)
O17−Mn1−N23	89.71(9)	N23−Mn1−N23a	162.98(7)	O6A−Mn1−O17	89.53(14)
O17−Mn1−N43	89.80(9)			O6A−Mn1−O37	91.57(14)
O37−Mn1−N23	88.63(9)			O6A−Mn1−N23	96.00(14)
O37−Mn1−N43	88.27(9)			O6A−Mn1−N43	87.46(13)
N23−Mn1−N43	163.47(8)			O17−Mn1−O37	178.49(9)
				O17−Mn1−N23	90.56(8)
				O17−Mn1−N43	88.32(8)
				O37−Mn1−N23	90.36(8)
				O37−Mn1−N43	90.69(8)
				N23−Mn1−N43	176.36(10)

[a] Symmetry operation: $1 - x, y, 1/2 - z$. [b] Major disorder component; occupation factor Br1A is 0.945(1). [c] Major disorder component; occupation factor O6A is 0.760(5).

Fourier methods (using DIRDIF99[29] for compounds **R-2** and **R-4**). Refinement on F^2 was performed with SHELXL-97.[30] The bromide ligand of structure **R-1** is disordered over two sites on opposite faces of the MnN_2O_2 coordination plane. The disorder ratio refined to 0.945(1):0.055. Structure **R-2** displayed disorder in the ethanol ligand and one of the OMe groups; the disorder ratios refined to 0.760(4):0.240 and 0.51(3):0.49, respectively. One of the $[H_2NEt_2]^+$ ions in the structure of **R-4** displays a slight conformational disorder in a refined ratio of 0.675(6):0.325. The $[HNEt_3]^+$ ion in the structure of **RS-5** is disordered over a crystallographic inversion center. The alkoxyl hydrogen atom of **R-2** was positively identified on a difference Fourier map. All hydrogen atoms, including the alkoxyl hydrogen of **R-2**, were included in calculated positions riding on their carrier atoms. All major component non-hydrogen atoms were refined with anisotropic displacement parameters. The absolute configuration of structures **R-1**, **R-2**, and **R-4** is confirmed by the value of the Flack *x* parameter,[31] obtained during the final structure-factor calculation. Neutral atom scattering factors and anomalous dispersion corrections were taken from the International Tables for Crystallography.[32] Validation, geometrical calculations, and illustrations were performed with PLATON.[26]

Results and Discussion

Syntheses. The chiral ligand *R*-HphoxCOOMe and the racemic ligand *RS*-HphoxCOOMe were synthesized, starting from the hydrochloride salts of *R*-serine methyl ester or *RS*-serine methyl ester, according to the reported procedure in good yields and purity.[24] However, on several occasions the oxazoline ring was found to be hydrolyzed as identified by the ESI-MS analysis. Observation of such hydrolyzed products has also been reported by Mugesh et al.,[33] who suggested that the ring opening was caused by metal-assisted hydrolysis in the presence of acetic acid. The relative amount of ring-opened products was higher in the synthesis of the ligand HphoxCOOH than that for HphoxCOOMe, probably because of the acid hydrolysis step. The reactions of the enantiopure (*R*) or racemic (*RS*) ligand HphoxCOOMe with Mn(II) salts easily resulted in the formation of pure crystalline green products.

The reaction of Mn(II) chloride or Mn(II) perchlorate with *R*-HphoxCOOH or *RS*-HphoxCOOH initially did not result in a color change. Upon addition of triethylamine, the solutions initially show a white precipitate, which dissolves, and the solutions turn green in a few minutes with stirring. The counteranion, protonated diethylamine, present in complex **R-4** most probably results from the decomposition of triethylamine in the reaction mixture.

Molecular Structures of [Mn(*R*-phoxCOOMe)$_2$Br] (R-1), [Mn(*R*-phoxCOOMe)$_2$Br][Mn(*S*-phoxCOOMe)$_2$Br] (RS-1), and [Mn(*R*-phoxCOOMe)$_2$(ClO$_4$)(EtOH)] (R-2). Crystallographic data for all the structures are collected in Table 1. Relevant bond distances and angles for complexes **R-1**, **RS-1**, and **R-2** are collected in Table 2. ORTEP projections of **R-1**, **RS-1**, and **R-2** are shown in Figures 2−4, respectively. Compounds **R-1** and **R-2** crystallize in the space group $P2_1$. Complex **RS-1** crystallizes in the centrosymmetric space group $C2/c$ with the manganese and bromide ions residing on a 2-fold rotation axis. The location of this axis ensures that each complex in the unit cell contains two ligands of the same chirality, either [Mn(*R*-phoxCOOMe)$_2$Br] or [Mn(*S*-phoxCOOMe)$_2$Br] (shown in Figure 3). Space-group symmetry ensures that these complexes are present in the crystal in a 1:1 ratio. In both **R-1** and **RS-1**, the manganese(III) ion is in an N_2O_2Br chromophore and has

(29) Beurskens, P. T.; Admiraal, G.; Beurskens, G.; Bosman, W. P.; García-Granda, S.; Gould, R. O.; Smits, J. M. M.; Smykalla, C. *The DIRDIF99 Program System*; Crystallography Laboratory, University of Nijmegen: Nijmegen, The Netherlands: 1999.
(30) Sheldrick, G. M. *SHELXL-97: Program for Crystal Structure Refinement*; University of Göttingen: Göttingen, Germany, 1997.
(31) Flack, H. D. *Acta Crystallogr. A* **1983**, *39*, 876−881.
(32) Wilson, A. J. C. *International Tables for Crystallography*; Kluwer Academic Publishers: Dordrecht, The Netherlands, 1992; Volume C.
(33) Mugesh, G.; Singh, H. B.; Butcher, R. J. *Eur. J. Inorg. Chem.* **2001**, 669−678.

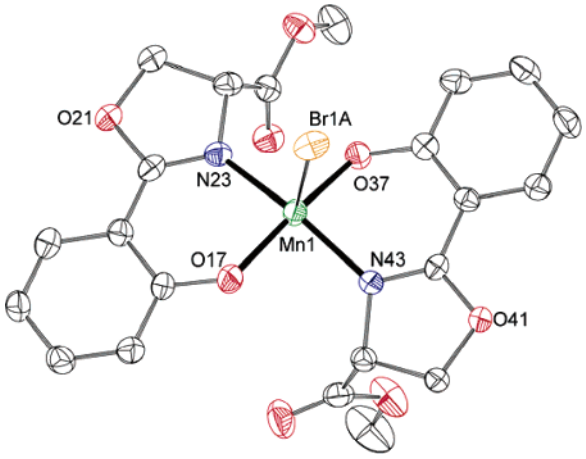

Figure 2. ORTEP plot at the 50% probability level of the [Mn(*R*-phoxCOOMe)$_2$Br] (**R-1**) complex. Hydrogen atoms are omitted for clarity.

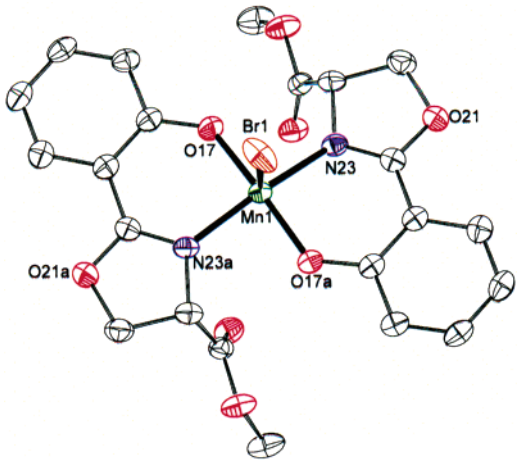

Figure 3. ORTEP plot at the 50% probability level of the {Mn(*R*-phoxCOOMe)$_2$Br}{Mn(*S*-phoxCOOMe)$_2$Br} (**RS-1**) complex showing the [Mn(*S*-phoxCOOMe)$_2$Br] molecule. Hydrogen atoms are omitted for clarity.

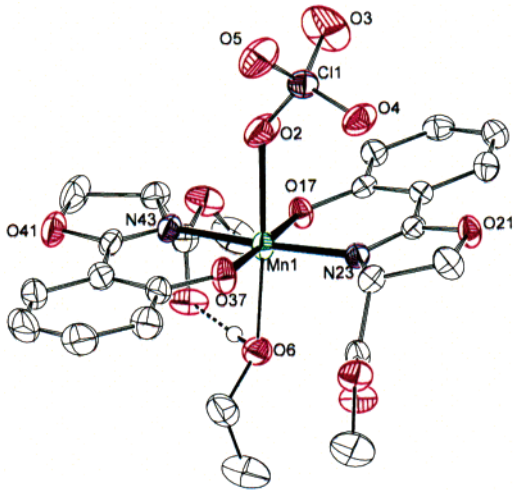

Figure 4. ORTEP plot at the 50% probability level of the [Mn(*R*-phoxCOOMe)$_2$(ClO_4)(EtOH)] (**R-2**) complex showing the major disorder component. Hydrogen atoms, except those attached to ethanol, are omitted for clarity.

square-pyramidal geometry. The τ parameter for **R-1** is 0.07, and for **RS-1**, it is 0.04, supporting the square-pyramidal geometry.[34] In all three structures, the two ligands are coordinated in the basal plane with like atoms in *trans*

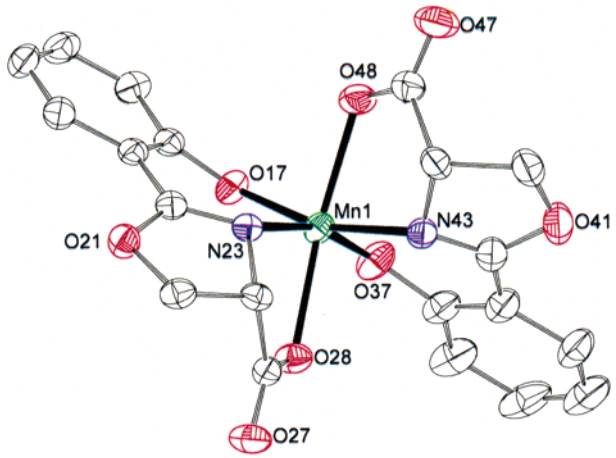

Figure 5. ORTEP plot at the 50% probability level of the anion of **R-4**. Hydrogen atoms are omitted for clarity.

positions. The three independent Mn−O bond lengths are around 1.86 Å, while the Mn−N bond lengths are close to 1.99 Å, typical for Mn(III) distances.[35,36] The Mn−O distances are significantly shorter than those in the [Mn(*R*-phox)$_3$] complexes (1.89 Å).[23,35] In **R-1** and **RS-1**, the manganese(III) ion is slightly above the plane formed by the phenoxo oxygens and oxazoline ring nitrogens, as expected for a square-pyramidal geometry; the displacements of the manganese ion from the least-squares plane formed by O17−N23−O37−N43 are 0.2443(4) Å and 0.2629(4) Å in complexes **R-1** and **RS-1**, respectively. A bromide ion is coordinated at the apical position at 2.5708(5) (**R-1**) and 2.550(6) Å (**RS-1**) on the Jahn−Teller axis (JT axis). In the complex **R-1**, the bromide ion is disordered over the two apical positions on the JT axis while in complex **RS-1** it is completely ordered. Remarkably, in complex **RS-1**, the racemic mixture of the ligand, *RS*-phoxCOOMe is separated into pure enantiomeric ligands to form a diastereomeric mixture of manganese complexes with chirally pure ligands instead of the expected *meso* complex, [Mn(*R*-phoxCOOMe)-(*S*-phoxCOOMe)Br].

The crystal structure of complex **R-2** is similar to that of complex **R-1**, except that an ethanol molecule and a perchlorate anion occupy two axial positions on the JT axis completing an octahedral coordination. The ester groups on both ligands are close to the coordinated ethanol molecule. There are strong hydrogen bonds between the carbonyl oxygens and the ethanol molecule that is disordered over two positions. The details of hydrogen bonding interactions are given in the Supporting Information (Table S1).

Molecular Structure of (H_2NEt_2) *fac*-cct-[Mn(*R*-[phox-COO)$_2$] (R-4). An ORTEP projection of the anionic complex **R-4** is shown in Figure 5. The crystallographic data are presented in Table 1. Selected bond distances and angles are given in Table 3. The crystal structure displays a complex

(34) Addison, A. W.; Rao, T. N.; Reedijk, J.; van Rijn, J.; Verschoor, G. C. *J. Chem. Soc., Dalton Trans.* **1984**, 1349−1356.
(35) Hoogenraad, M.; Ramkisoensing, K.; Kooijman, H.; Spek, A. L.; Bouwman, E.; Haasnoot, J. G.; Reedijk, J. *Inorg. Chim. Acta* **1998**, *279*, 217−220.
(36) Shyu, H. L.; Wei, H. H.; Wang, Y. *Inorg. Chim. Acta* **1999**, *290*, 8−13.

Table 3. Selected Bond Distances (Å) and Angles (deg) for Complexes **R-4** and **RS-5**

R-4[a]			**RS-5**[b]	
Mn1−O17	1.8722(19)	1.8856(18)	Mn1−O1	2.2397(17)
Mn1−O28	2.2337(19)	2.2356(19)	Mn1−O17	1.8734(14)
Mn1−O37	1.8918(18)	1.8788(16)	Mn1−N23	2.0120(18)
Mn1−O48	2.2584(19)	2.2867(19)		
Mn1−N23	2.002(2)	1.9960(19)		
Mn1−N43	2.000(2)	2.012(2)		
O17−Mn1−O28	104.96(8)	110.87(7)	O1−Mn1−O17	91.86(7)
O17−Mn1−O37	91.57(8)	90.24(7)	O1−Mn1−N23	89.46(7)
O17−Mn1−O48	88.35(8)	88.45(7)	O17−Mn1−N23b	89.13(7)
O17−Mn1−N23	90.37(8)	89.91(8)	O17−Mn1−N23	90.87(7)
O17−Mn1−N43	162.31(9)	160.75(9)	O1−Mn1−O17b	88.14(7)
O28−Mn1−O37	87.67(8)	88.62(7)	O1−Mn1−N23b	90.54(7)
O28−Mn1−O48	159.38(7)	155.67(7)		
O28−Mn1−N23	74.36(8)	75.28(8)		
O37−Mn1−O48	107.98(8)	106.55(7)		
O37−Mn1−N23	161.80(9)	162.80(9)		
O37−Mn1−N43	90.09(8)	90.32(8)		
O48−Mn1−N23	90.17(8)	90.65(8)		
O48−Mn1−N43	74.41(8)	72.97(8)		
N23−Mn1−N43	93.53(8)	95.15(8)		

[a] For **R-4**, two values are cited for each parameter. The first number is the parameter cited in the table. The second number is the value of the related geometric parameter in the independent complex containing Mn2. [b] Symmetry operation: $2 - x, 1 - y, 1 - z$.

of manganese(III) with two *R*-phoxCOO^{2-} ligands, deprotonated at both the phenol and carboxylic acid moieties. The ligands are coordinated to the manganese ion in a tridentate manner through the phenolate oxygen atom, oxazoline nitrogen atom, and one of the carboxylate oxygen atoms. The asymmetric unit consists of two crystallographically independent manganese complexes, which have virtually the same geometry, as is clear from the data in Table 3. The asymmetric unit also contains two protonated diethylamine ($H_2NEt_2^+$) ions, which balances the negative charge on the complex molecules. The manganese(III) ion is in a highly distorted octahedral geometry in a N_2O_4 chromophore. The two ligands are attached to the manganese ion in a facial fashion with the phenolate and oxazoline donors in mutual *cis* positions in the equatorial plane. The two carboxylate groups occupy the axial positions, the angle O28−Mn1−O48 being 159.38(7)°, showing significant deviation from the normal 180° value. Because of the coordination of the carboxylate groups on the ligands, the plane containing the phenol and the oxazoline groups on the ligands is highly distorted from the planar geometry, the dihedral angles between the phenol ring and the oxazoline ring on the ligands being 25.08(16)° and 21.09(13)° in the molecule containing Mn1 and 27.48(41)° and 25.97(12)° in the molecule containing Mn2. As a result, the square plane around manganese is also distorted, and the dihedral angle between the planes Mn1−O17−N23 and Mn1−O37−N43 of 25.40(12)° shows a large deviation from the ideal planarity; the corresponding parameter for Mn2 is 25.64(12)°. The Mn−O (phenolate) distances are longer (1.8722(19)−1.8914(18) Å) than the corresponding distances in the Mn−phoxCOOMe complexes described above (**R-1**, **RS-1**, and **R-2**). The Mn−N and Mn−O (axial carboxylate) distances are similar to those observed in other Mn(III) complexes.[21−23,35,36] The hydrogen bonds donated by the diethylammonium protons to the

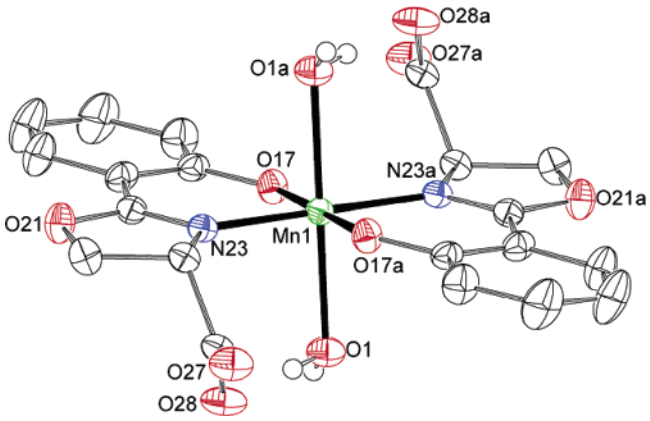

Figure 6. ORTEP plot at the 50% probability level of the *trans*-[Mn(*R*-phoxCOO)(*S*-phoxCOO)$(H_2O)_2$]$^-$ (**RS-5**) anion. The cation and hydrogen atoms (except those attached to water molecules) are omitted for clarity.

carboxylate groups of the manganese complexes link the molecules into infinite one-dimensional chains running parallel to the *a* axis. Details of the hydrogen bonding interactions are given in the Supporting Information (Table S1).

Molecular structure of (HNEt$_3$) *trans*-[Mn(*RS*-phoxCOO)$_2$(H$_2$O)$_2$] (RS-5). An ORTEP projection of the molecule of the complex ion is shown in Figure 6. The crystallographic data are presented in Table 1, and selected bond distances and angles are given in Table 3. The crystal structure shows a complex of manganese(III) with two enantiomers of the ligand, with the manganese ion located on a crystallographic inversion center. The ligands, deprotonated at both the phenol and the carboxylic acid moieties, are bound in a *trans* fashion through the phenolate oxygen and the oxazoline nitrogen atoms in a didentate manner. The carboxylate groups are not coordinated to the metal center; instead, two water molecules occupy the remaining two axial sites of the manganese ion along the JT axis. The Mn−O (phenolate) distance is 1.8734(14) Å, while the Mn−N distance is 2.0120(18) Å. The dihedral angle between the phenol and oxazoline rings is 5.64(13)°, showing a nearly planar system, as opposed to the strong distortion in **R-4**; this is an obvious observation as the ligands are not forced to the distortion by carboxylate coordination. The crystal structure contains a protonated triethylamine ($HNEt_3^+$) molecule to (counter) balance the overall negative charge of the Mn complex. Strong hydrogen bonding interactions assemble chains of complex molecules in the crystal lattice, as shown in Figure 7. Details of the hydrogen bonding interactions are given in the Supporting Information (Table S1). The carboxylate groups on each ligand form an intramolecular hydrogen bond to the water molecule. The water molecule on the neighboring complex is perfectly placed for intermolecular hydrogen bonding with the second oxygen on the carboxylate groups, and thus, the molecules form a one-dimensional infinite chain parallel to the *a* axis. The disordered triethylammonium ions donate, in both orientations, a hydrogen bond to a carboxylate group.

Spectroscopic Data. All complexes display ligand field bands that are very similar in position. The shoulder at around 440−450 nm (ϵ = 800−1100 M^{-1} cm^{-1}) may be the result

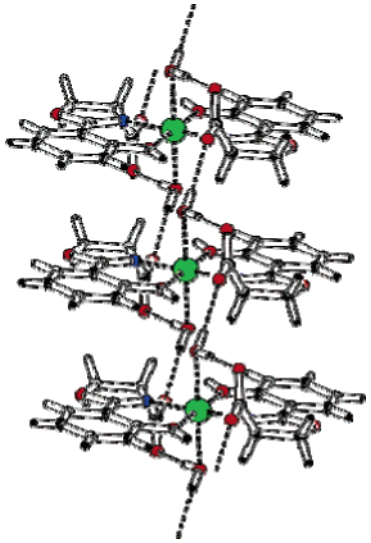

Figure 7. PLUTON projection of the hydrogen bonding network in complex **RS-5**.

of mixing of an LMCT band and a d−d transition.[37−39] The broad band centered around 600 nm (ϵ = 200−250 M^{-1} cm^{-1}), extending to 800 nm, can be assigned to a d−d transition.[39]

For all complexes, the parent peak observed in the positive mode ESI-MS spectra originates from the $[MnL_2]^+$ fragment with, for some of the complexes, a secondary peak assigned to $[MnL_2(solvent)]^+$. The ESI-MS analysis of complex **R-1** or **RS-1** in acetone solution gives two major peaks at *m*/*z* 495 (I = 100%) and 553 (I = 40%) assigned to $[Mn^{III}(phoxCOOMe)_2]^+$ and $[Mn^{III}(phoxCOOMe)_2(acetone)]^+$, respectively. In addition, a low-intensity peak is observed at *m*/*z* 1070 ($I \approx 1\%$). This peak can be tentatively assigned to $[Mn^{III}(phoxCOOMe)_2\text{-}Br\text{-}Mn^{III}(phoxCOOMe)_2]^+$. Formation of such a dinuclear species in low amounts in solutions containing the [Mn(salen)Cl] complex using ESI-MS analysis has recently been reported.[40] For complexes **R-2** and **RS-3**, similar low intensity peaks are observed at 1089 for $[\{Mn^{III}(phoxCOOMe)_2\}_2(ClO_4)]^+$.

Positive and negative ion ESI-MS analysis was used for the characterization of complexes **R-4** (MeOH) and **RS-5** (acetone) (Figures S1−S4). In negative ion ESI-MS, for both complexes, peaks are observed at *m*/*z* 465 (I = 100% for **R-4** and **RS-5**) assigned to the $[Mn^{III}(phoxCOO)_2]^-$ fragment. In positive ion ESI-MS, the peak for the $[Mn^{III}(phoxCOOH)_2]^+$ fragment was observed for both complexes at *m*/*z* 467, wherein both ligands are monoanionic. In addition, for complex **RS-5**, a peak at *m*/*z* 525 (I = 70%) is also observed and assigned to $[Mn^{III}(phoxCOOH)_2(acetone)]^+$. The assignment of the peaks is supported by excellent fitting of the isotope patterns.

The racemic ligand *RS*-HphoxCOOMe exhibits strong characteristic IR absorptions for the ester carbonyl group at 1740 cm^{-1}. The strongest absorptions are in the range of 1690−1636 cm^{-1}, and they can be assigned to the stretching vibrations of the unsaturated C═N and C═C linkages in the ligand.[41] Weak absorptions between 3000 and 2920 cm^{-1} are assigned to the symmetric and antisymmetric stretching vibrations of the oxazoline ring alkyl protons.[42] The IR spectra of complexes **R-1**, **RS-1**, **R-2**, and **RS-3** show the C═O vibration at around 1748 cm^{-1}. The C═N and C═C stretching vibrations appear between 1585 and 1610 cm^{-1} for all complexes, which is a shift of about 20 cm^{-1} from that of the free ligand, indicating coordination of manganese. For complex **R-2**, the perchlorate vibration appears as a doublet of peaks at 1090 and 1031 cm^{-1}, indicating coordination of the perchlorate group as opposed to the singlet peak at 1089 cm^{-1} in the IR of **RS-3**, indicating noncoordinated perchlorate. In complex **RS-3**, one or two molecules of water could be coordinated instead, as indicated by the elemental analyses.

The peak of C═O at 1694 cm^{-1} present in the free ligand HphoxCOOH is absent in complexes **R-4** and **RS-5** indicating coordination of the ligand and suggesting that either the two oxygens on the carboxylate group are equivalent as in **RS-5** or the carbonyl oxygen participates in coordination to the metal as in **R-4**. In addition, the C═N vibrations are shifted to 1608 and 1615 cm^{-1} for complexes **R-4** and **RS-5**, respectively, confirming coordination of the metal to the ligand. The lower value for **R-4** suggests a weaker C═N bond consistent with the distortion of the oxazoline ring with respect to the phenyl ring which reduces the resonance stabilization of the C═N bond. The C═C vibrations are observed at around 1585 cm^{-1} for both the complexes. Broad peaks in the 3000−3300 cm^{-1} region resulting from the presence of hydrogen-bonded ethylammonium cations are also present in the IR spectra of the two complexes.

For all complexes, the Mn(III) oxidation state is in accordance with the absence of an EPR signal at 77 K and at room temperature and with the magnetic susceptibility data at room temperature ranging from 4.50 to 4.8 μ_B. These data are close to the spin-only value of 4.92 μ_B for high-spin manganese(III), the deviation being caused by orbital effects.[43] The specific conductivity of 1 mM solutions of the complexes has been measured in methanol. The values for the molar conductivity for all complexes vary from 79 to 96 Ω^{-1} cm^2 mol^{-1}, suggesting that the complexes exist as 1:1 electrolytes in solution.[44] Thus, the coordinating anions of complexes **R-1**, **RS-1**, **R-2**, and **RS-3** dissociate in solution, in agreement with the ESI-MS data.

The redox behavior of the complexes was studied by cyclic voltammetry (CV). The potentials are given against Ag/AgCl.

(37) Marappan, M.; Narayanan, V.; Kandaswamy, M. *J. Chem. Soc., Dalton Trans.* **1998**, 3405−3409.
(38) Neves, A.; Erthal, S. M. D.; Vencato, I.; Ceccato, A. S.; Mascarenhas, Y. P.; Nascimento, O. R.; Horner, M.; Batista, A. A. *Inorg. Chem.* **1992**, *31*, 4749−4755.
(39) Boucher, L. J.; Day, V. W. *Inorg. Chem.* **1977**, *16*, 1360−1367.
(40) Chipperfield, J. R.; Clayton, J.; Khan, S. A.; Woodward, S. *J. Chem. Soc., Dalton Trans.* **2000**, *7*, 1087−1094.
(41) Lin-Vien, D.; Colthup, N. B.; Fateley, W. G.; Grasselli, J. G. *The Handbook of Infrared and Raman Characteristic Frequencies of Organic Molecules*; Academic Press Limited: London, 1991; p 200.
(42) Socrates, G. *Infrared Characteristic Group Frequencies*; John Wiley and Sons: Bath, U.K., 1980; p 3.
(43) Drago, R. S. *Physical Methods in Inorganic Chemistry*; Reinhold Publishing Corporation: New York, 1965; pp 389−397.
(44) Geary, W. J. *Coord. Chem. Rev.* **1971**, *7*, 81−122.

The cyclic voltammograms of the complexes are given in the Supporting Information (Figures S5− S10). The cyclic voltammograms of **R-1**, **R-2**, **RS-1**, and **RS-3** show very similar patterns. The complexes display a well-defined quasi-reversible wave around 0.08−0.04 V ($E_{1/2}$) in the cathodic scan. The peak-to-peak separations (ΔE) for the process are around 130−180 mV, and it is diffusion controlled as the ratio of the current (i_{pa}) versus the square root of the scan rate ($\nu^{1/2}$) is constant in a range of scan rates from 0.025 to 0.5 V/s. In the same conditions, a reversible oxidation of ferrocene is observed at 0.04 V with a peak-to-peak separation of 95 mV. The cyclic voltammograms for the complexes **RS-5** and **R-4** are more complex with quasi-reversible oxidation and reduction peaks ($\Delta E \approx 120-180$ mV). However, the positions as well as the peak-to-peak separations change with scan rate, and detailed electrochemical studies are necessary for their correct assignments.

Paramagnetic Proton NMR. Paramagnetic ^{1}H NMR spectra of the new complexes in CD_3OD have aided in elucidating the solution chemistry of these complexes. The NMR studies of complex **R-4** are excluded from this discussion because this complex shows a complex uninterpretable ^{1}H NMR spectrum caused by its lack of symmetry. As a result of the C_2 or C_i symmetry of the other complexes in solution, the ^{1}H NMR spectra show only one set of signals for the two ligands in a complex molecule. Representative ^{1}H NMR spectra (recorded with a normal pulse sequence) of the complexes are presented in Figure 8. Inversion-recovery pulse sequence experiments were performed for complexes **RS-1** and **RS-5**. The results appeared to be very similar; the results for **RS-1** are given in Figure 9, and those for **RS-5** are given in the Supporting Information (Figure S11).

The spectra typically show signals ranging from +25 to −30 ppm, with diamagnetic signals from the solvents between 0 and 10 ppm. The complete ^{1}H NMR spectroscopic data and tentative assignments for all complexes except **R-4** are collected in Table 4. The ^{1}H NMR spectrum of **R-1** and **RS-1** clearly show isotropically shifted signals; three signals at low field (23.7, 14.8, and 12.8 ppm) and three signals at high field (−10.8, −23.1, and −27.1 ppm). The latter two resonances have relatively large relaxation values, corresponding with the fact that these two hydrogen atoms of the phenolate ring are relatively far away from the Mn atom. Previous studies performed on substituted Mn−phox complexes[21] have shown that one of the upfield signals (at about −26.4 ppm) is absent in the chloro-substituted complex, $[Mn(5'\text{-Clphox})_2(MeOH)_2]^+$.[21] Literature data[21,45−47] show that the relatively sharp signals from −15 to −30 ppm can be assigned to the H4′ and H5′ hydrogen atoms of the phenolate ring. Lamar et al. have reported that for Mn(III) compounds the major contribution to the isotropic shift is made by the contact shift.[48,49] Thus, corresponding to distances found in the X-ray crystal structure of **RS-1** (Mn−H4′ (6.127 Å) < Mn−H5′ (6.505 Å)) and the relaxation time for the H4′ signal of **RS-1** is expected to be shorter than that of H5′. Therefore, the signal at −23.1 ppm is tentatively assigned to H4′ of the phenolate ring of **RS-1**, and the signal at −27.1 ppm is assigned to H5′.

The signal at −10.8 ppm is very broad, has a short relaxation time, and can be assigned to H6′ or H3′. X-ray data of **RS-**1 show that the distance of H3′−Mn is shorter than that of H6′−Mn (Mn1−H3′ = 4.365 and 4.268 Å and Mn1−H6′ = 5.336 and 5.229 Å for the two ligands). The resonance of H3′ is probably too broad to be detected because of the closeness to the Mn center, as was also observed in case of the Mn−phox complexes studied earlier.[21] In addition, the H6′ and H4′ protons are both four bonds away from the manganese ion. From X-ray data, the distance Mn−H6′ is shorter than Mn−H4′ (Mn1−H4′= 6.127 Å). Thus, the peak of the H6′ proton is expected to be broader and the relaxation time is expected to be lower compared to those of the H4′ proton. Therefore, the resonance at −10.8 ppm is tentatively assigned to H6′.

By substituting one of the protons at the C4 atom with an ester or carboxylic acid substituent, the signals of the H4 and H5 protons of complex **RS-1** can now be differentiated, compared to those of the ^{1}H NMR of the $[Mn(phox)_2(MeOH)_2]^+$ complex.[21] The spectrum of **RS-1** shows three signals in the downfield region. The signal at 27.7 ppm is tentatively assigned as H4, and the two signals at 14.8 and 12.8 ppm are assigned as H5a and H5b. When an inversion-recovery pulse sequence of $T_1 = 1$ ms was applied to complex **RS-1** in CD_3OD, all signals from the solvent (diamagnetic) are negative and the paramagnetic peaks (from the complex) are positive (Figure 9). The signal for the methyl protons from the ester groups is visible in this spectrum, and the intensity of this signal is three times higher than the intensity of H4′. The assignment of this signal to the methyl protons is further confirmed by the fact that the peak shows the broadened features of a paramagnetic signal in contrast to the sharp solvent signals (∼4 ppm) and the absence of this signal in the corresponding MnphoxCOO complex (**RS-5**). Moreover, the ^{1}H NMR of **R-1** in acetonitrile clearly shows the signal of CH_3 at 4 ppm (Figure 8E). The ^{1}H NMR spectrum of complexes **RS-3** and **RS-5** are essentially the same, and for the assignment, the same reasoning as above can be applied. The reason for the splitting of the resonance of H5′ in both **RS-1** and **RS-3** is not clear.

Epoxidations. The complexes were tested in catalytic oxidations of various substrates in acetone/methanol mixtures at 0 °C. A known amount of additive and alkene was added to a catalyst solution, followed by an excess of dihydrogen peroxide solution. When all of the H_2O_2 is added at once, vigorous decomposition of dihydrogen peroxide is observed, as a result of a catalase-type reaction, resulting in low yields

(45) Bermejo, M. R.; Gonzalez-Noya, A. M.; Abad, V.; Fernandez, M. I.; Maneiro, M.; Pedrido, R.; Vazquez, M. *Eur. J. Inorg. Chem.* **2004**, 3696−3705.
(46) Bonadies, J. A.; Maroney, M. J.; Pecoraro, V. L. *Inorg. Chem.* **1989**, *28*, 2044−2051.
(47) Ciringh, Y.; Gordon-Wylie, S. W.; Norman, R. E.; Clark, G. R.; Weintraub, S. T.; Horwitz, C. P. *Inorg. Chem.* **1997**, *36*, 4968−4982.
(48) Wu, F. J.; Kurtz, D. M.; Hagen, K. S.; Nyman, P. D.; Debrunner, P. G.; Vankai, V. A. *Inorg. Chem.* **1990**, *29*, 5174−5183.
(49) Lamar, G. N.; Eaton, G. R.; Holm, R. H.; Walker, F. A. *J. Am. Chem. Soc.* **1973**, *95*, 63−75.

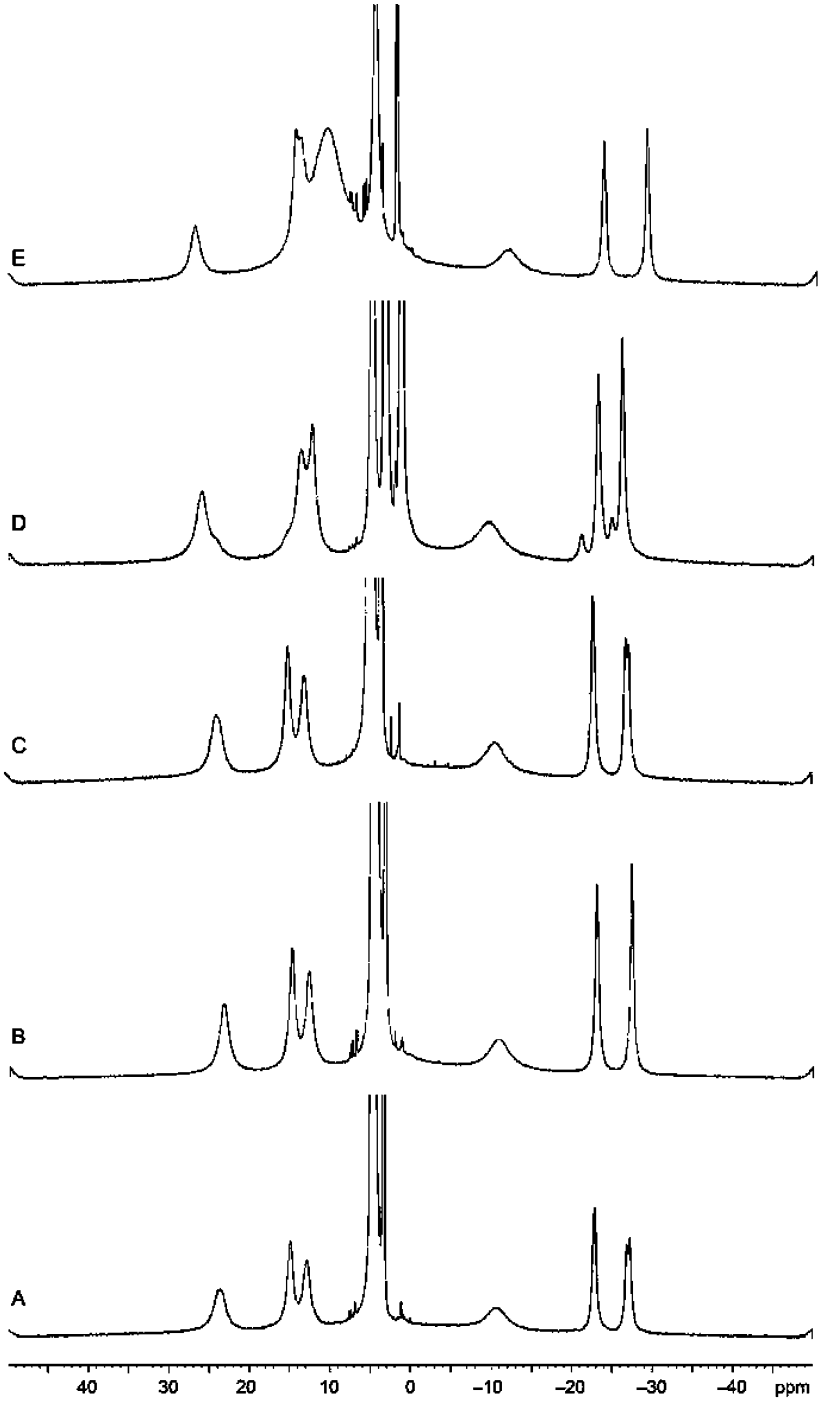

Figure 8. ^{1}H NMR of the complexes: (A) **RS-1** (MeOD), (B) **R-1** (MeOD), (C) **RS-3** (MeOD), (D) **RS-5** (MeOD), and (E) **R-1** (CD_3CN).

of the epoxide product. The green solutions slowly turn brown on addition of H_2O_2 and then turn yellow/colorless after a few minutes. The catalytic activity, however, continues for 3−5 h. The difference in turnover numbers that can be reached using different solvents (viz., acetone, methanol, and acetonitrile) in the oxidation of styrene by complex **RS-1** is not large, although the use of acetone results in slightly higher turnover numbers. The use of acetone in combination with H_2O_2 is known to yield perhemiketal adducts that slowly release H_2O_2 during reaction.[50] Thus, acetone has been the solvent of choice for the epoxidation studies. However, it was found that a mixture of acetone/MeOH in an 80:20 ratio (v/v) works best; methanol is necessary for good solubility of the complexes.

Several additives were screened in combination with **R-1** and **RS-1** for optimization of the activity of the catalysts. A summary of the results obtained with various additives is given in Table 5. No epoxide product is formed in both cases in the absence of an additive (entry 1). In general, all imidazole-type additives result in improved conversions (entries 2−5). However, the addition of other nitrogen-containing bases, such as pyrazole, pyridine, and pyridine *N*-oxide

(50) Sauer, M. C. V.; Edwards, J. O. *J. Phys. Chem.* **1971**, *75*, 3004−3011.

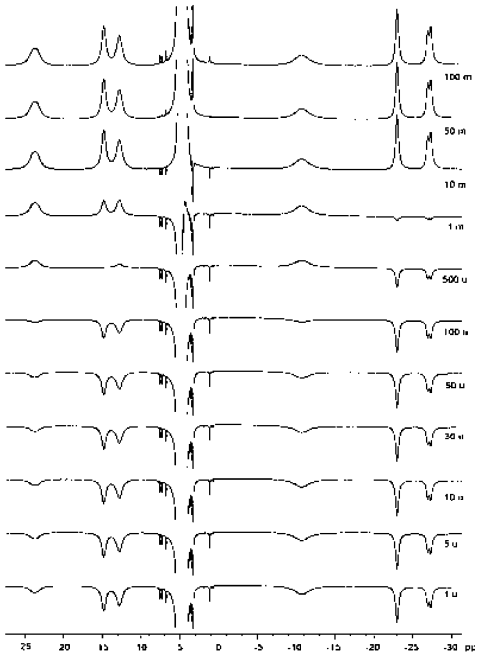

Figure 9. ^{1}H NMR spectra obtained with the inversion-recovery pulse sequence for complex **RS-1** in CD_3OD.

(entries 7−9), did not result in any enhanced catalytic activity. Looking at the pK_b values for the two additives, imidazole and pyridine, a simple calculation for *aqueous* solutions shows that 100× more pyridine would be required to achieve roughly the same pH as that of an imidazole solution. The epoxidation experiments have also been performed with 100 and 1000 equiv of pyridine, but even with these amounts, no epoxide product is formed. However, the consideration of pH effects is not quite valid for the organic medium as used in our catalytic studies; it is therefore questionable whether the same "pH" is reached in both cases. Acetic acid was tested at 0 °C as well as at room temperature (entry 10). On addition of dihydrogen peroxide to a green solution containing the catalyst, acetic acid, and the alkene, the solution turns colorless and no catalase activity is observed. However, epoxidation activity is also not observed using acetic acid as additive. The use of ascorbic acid also resulted in no activity in both complexes, **R-1** and **RS-1** (entry 11). The use of sodium acetate and ammonium acetate resulted in 12 and 15 turnovers to styrene epoxide in complex **R-1** and 32 and 29 turnovers in complex **RS-1** (entries 12, 13). $NaHCO_3$ was also tested as an additive, and maximum turnovers resulted with 10 equiv $NaHCO_3$ for both **RS-1** and **R-1** (entry 14).

It is clear from the results given in Table 5 that the epoxidation activity is directly dependent on the basicity of the additives used and a minimum basicity of the additive is necessary to achieve at least some enhanced catalytic activity. Whereas pyridine and pyridine-*N*-oxide with p*K* values of 5.25 and 0.79 do not enhance the catalytic activity, all imidazole additives (p*K* values typically above 6) do enhance the catalytic activity. It is important to note the difference in activity between the complexes **RS-1** and **R-1**; surprisingly the use of **RS-1** results in significantly higher turnover numbers than the use of **R-1**. In the styrene epoxidations, phenyl acetaldehyde (TON ≈ 2−9) was found to be the main side product instead of the usually observed side product, benzaldehyde.[23,35,51] An interesting point to note here is that, for the epoxidation with imidazoles and acetate salts, marked similarities are found in the selectivity toward epoxide and formation of the byproduct phenyl acetaldehyde. Control experiments showed that phenyl acetaldehyde does not result from the reaction of styrene oxide with the catalyst. The turnovers of phenyl acetaldehyde are higher in the case of **RS-1** as compared to that in **R-1**, in accordance with the higher conversion.

To widen the substrate scope, the complexes have been tested in the catalytic epoxidation of various alkenes (Table 6). The yields of the product are higher for all olefins when using the *meso* complexes **RS-1** and **RS-3** than when using the enantiopure complexes **R-1** and **R-2**, with the corresponding epoxide being the major product in all cases.

Of the substrates tested, cyclohexene results in the highest conversion. In general, the complexes show comparable conversion for cyclooctene and 1-octene, the exception being **RS-1**, for which the turnovers in cyclooctene (30) are considerably higher than for 1-octene (22). Important to note here is the epoxidation of 1-octene, for which 10 to 23 turnovers in the epoxide product were obtained by the above complexes. The linear chain alkenes such as 1-octene are known to be more difficult to oxidize than the cyclic alkenes.[9,52] For alkenes other than styrene, no side products were observed in detectable amounts.

The **R-4** and **RS-5** complexes have also been tested as catalysts for the epoxidation of various substrates. In the absence of *N*-Meim, these complexes do not show any catalytic activity. Low conversions (up to 10 turnovers) are obtained in the oxidation of styrene; for the other substrates no conversion is obtained at all. The low activity of the phoxCOO complexes may be attributed to the presence of the (potentially) coordinating carboxylate group. The presence of the chiral center in the oxazoline ring makes the complexes potential candidates for asymmetric catalysis. Preliminary studies using *R*(+)-limonene and styrene, however, showed only limited asymmetric induction and further studies have been abandoned.

ESI-MS Studies. Binding of *N*-Meim. The differences in the catalytic activities of complexes **RS-1** and **R-1** (and for complexes **RS-3** and **R-2**) were intriguing as the solid-state structures of complexes **RS-1** and **R-1** showed no structural differences. The chiral molecule of [Mn(*R*-phoxCOOMe)$_2$Br] present in **RS-1** is structurally the same as that in **R-1**; in addition, the X-ray structure of **RS-1** shows the presence of the other enantiomer, [Mn(*S*-phoxCOOMe)$_2$Br]. To elucidate the structures of the complexes in solution in the presence and absence of *N*-Meim, ESI-MS studies have been undertaken. The ESI-MS spec-

(51) Brinksma, J.; Hage, R.; Kerschner, J.; Feringa, B. L. *Chem. Commun.* **2000**, 537−538.
(52) Hoogenraad, M. Manganese Complexes as Catalysts for Homogeneous Oxidation Reactions. Ph.D. Thesis, Leiden University, Leiden, The Netherlands, 2000.

Table 4. ^{1}H NMR Chemical Shifts (ppm) and Tentative Assignments for Complexes **R-1**, **R-2**, **RS-1**, **RS-3**, and **RS-5**[a]

	δ (T_1/msec)					
	H4	H5	H6′	H4′	H5′	other peaks
R-1, and **RS-1**	23.7 (0.574)	14.8 (1.021), 12.8 (0.797)	−10.8 (0.308)	−23.1 (2.371)	−27.1 (2.744)	CH_3: 4.3 (1.522)
R-2, and **RS-3**	23.9	14.9, 12.9	−10.6	−22.9	−26.9	CH_3: 4.4
RS-5	25.9 (0.438)	13.7 (0.775), 12.2 (1.071)	−9.6 (0.169)	−23.2 (2.775)	−26.2 (3.253)	$HNEt_3$: 3.1 (21.0), 1.21 (19.5)
5[b]	19.6	13.4	−10.0	−22.0	−26.4	

[a] T1 values are given in parentheses; see Figure 1 for proton numbering. [b] **5** = $[Mn(phox)_2(MeOH)_2][Mn(phox)_2(ClO_4)_2](H_2O)_2$; taken from ref 21.

Table 5. Epoxidation of Styrene in the Presence of Various Additives with Complexes **R-1** and **RS-1**[a]

entry	additives	**R-1** TON[b]	**RS-1** TON
1	no additive	0	0
2	1-methyl imidazole	10 (1)	36 (6)
3	2-methyl imidazole	13 (4)	29 (7)
4	4-methyl imidazole	17 (4)	26 (5)
5	1, 2 dimethyl imidazole	12 (4)	26 (6)
6	imidazole	11 (2)	26 (5)
7	pyrazole	0	1
8	pyridine	0	1
9	pyridine *N*-oxide	0	1
10	acetic acid[c]	0	0
11	ascorbic acid	0	0
12	sodium acetate	12 (3)	33 (9)
13	ammonium acetate	14 (3)	30 (7)
14	sodium hydrogen carbonate	10 (2)	25 (6)

[a] Turnover numbers are for styrene epoxide obtained after 3 h. Values in parentheses indicate the turnover numbers obtained for the side product, phenyl acetaldehyde. Experimental conditions: (for details see the Experimental Section) cat/additive/alkene/H_2O_2 = 1:10:100:800, solvent = 80/20 acetone/MeOH, and temperature = 0 °C. [b] TON is turnover number of the epoxide product in moles of product per mole of catalyst. [c] The additive was tested for several equivalents from 1 to 500, with zero turnovers in all amounts (in acetone as well as acetonitrile).

Table 6. Turnover Numbers in the Oxidation of Various Alkenes by Complexes **R-1**, **RS-1**, **R-2**, and **RS-3**[a]

	R-1[b]	**RS-1**[b]	**R-2**[b]	**RS-3**[b]
styrene	10 (1)	36 (6)	15 (3)	32 (2)
cyclohexene	17	42	21	36
cyclooctene	10	30	11	21
1-octene	12	22	11	23

[a] Cat/ *N*-Meim/alkene/H_2O_2 = 1:10:100:800. Solvent: acetone/MeOH = 80:20. Temperature = 0 °C. Turnover numbers after 3 h. [b] Turnover number of the epoxide product in moles of product per mole of catalyst. The numbers in parentheses indicate turnover numbers for phenyl acetaldehyde.

trum of the complex **R-1** in the presence of 10 equiv of *N*-Meim (or pyridine) shows a peak that could be assigned to the $[Mn(phoxCOOMe)_2(N\text{-Meim})]^+$ fragment (*m*/*z* 577, *I* = 30%) (at *m*/*z* 574 for pyridine) in addition to the parent peak at *m*/*z* 495 of $[Mn(phoxCOOMe)_2]^+$. The solution of complex **RS-1** containing 10 or 100 equiv of *N*-Meim (or pyridine) does not show any signal assignable to a possible adduct. Only when *N*-Meim (or pyridine) is added in a very high excess (1000 equiv) is a peak of low intensity assignable to $[Mn(phoxCOOMe)_2(N\text{-Meim})]^+$ (*m*/*z* 577, *I* = 30%) observed for complex **RS-1** (likewise for pyridine). On the other hand, several attempts to synthesize the metal complex **RS-1** containing *N*-Meim as an additional ligand have failed. These ESI-MS results are unexpected as the reactivity of **R-1** and **RS-1** toward *N*-Meim is expected to be the same regarding the near identical X-ray crystal structures (Figures 2 and 3). These structures suggest that there is space for *N*-Meim to bind to the metal center at an apical site both in **R-1** and in **RS-1**.

To understand the results, the hypothetical complex [Mn(*R*-phoxCOOMe)(*S*-phoxCOOMe)]$^+$ is proposed as the solution structure of **RS-1** (Figure 10b). If in this structure the two ligands are bound in a *trans* fashion to the metal center, the ester groups are pointing in opposite directions along the axial sites, thus blocking the access of *N*-Meim to the metal center from both directions.

To support this hypothesis, ESI-MS studies of a mixture of deuterated (*S*-HphoxCOOCD$_3$) and undeuterated (*R*-HphoxCOOCH$_3$) ligands in combination with Mn(II) salts have been performed. A solution containing *S*-HphoxCOOCD$_3$, *R*-HphoxCOOCH$_3$, and Mn(II) perchlorate in methanol in a 1:1:1 ratio shows three major peaks in ESI-MS analyses. Peaks are observed at 495.06 (*I* = 75%), 498.07 (*I* = 100%), and 501.08 (*I* = 35%) and can be assigned to $[Mn(R\text{-phoxCOOCH}_3)_2]^+$, $[Mn(R\text{-phoxCOOCH}_3)(S\text{-phoxCOOCD}_3)]^+$, and $[Mn(S\text{-phoxCOOCD}_3)_2]^+$, respectively (Figure S12). These assignments are supported by excellent fitting of the isotope patterns. A comparison of the relative intensities of the peaks confirms that a complex of the type *R*−Mn−*S* is the major species in solution. On the basis of statistical factors, a ratio of 1:2:1 is expected for the three products. However, the ESI-MS intensities do not need to be strictly correlated with the actual relative concentrations in solution.[53] Additional experiments using *R*-phoxCOOMe, *S*-phoxCOOCD$_3$, $MnBr_2$ (1:1:1), and additional pyridine have also been carried out. At 10 and 100 equiv of pyridine, no adduct species are observed. With 1000 equiv of pyridine, a group of peaks assignable to $[Mn(L)_2(py)]$ for all three isomers is observed (*RR*, *RS*, and *SS*). This experiment shows that the *RS* complex can bind the additive but only at very high concentrations: concentrations that are 100-fold higher than those for the *R* complex.

It appears that in the crystal structure of **RS-1**, the racemic mixture of ligands is separated to two diastereomeric complexes, whereas when **RS-1** is dissolved, the *meso* type of complex is formed by the ligand-exchange equilibrium shown in Scheme 1. The X-ray crystal structure of **RS-5** confirms the possibility of such a *meso*-type complex. The results of the ESI-MS analyses, showing structural differences and reactivity toward nitrogen bases in solution, clearly can explain the observed differences in the catalytic activity between **RS-1** and **R-1** (and between **RS-3** and **R-2**).

Comparison to Other Systems. An interesting observation came to light during the epoxidation studies using

(53) Skoog, D. A. *Principles of Instrumental Analysis*; Saunders College Publishing: Philadelphia, PA, 1985; pp 523−566.

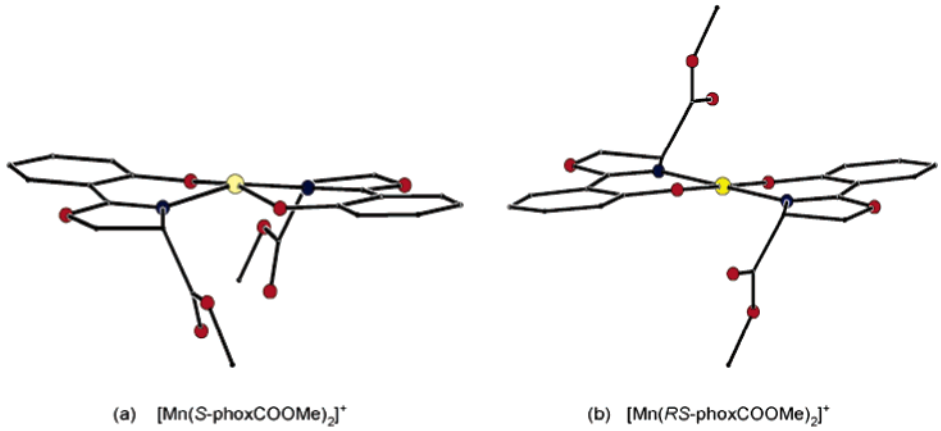

Figure 10. Schematic representation of the environment of the manganese ions with variation of the chirality of the ligand: (a) coordination of two ligands having same chirality and (b) coordination of two enantiomeric ligands.

Scheme 1. Ligand-Exchange Equilibrium Occurring in Complex **RS-1** in MeOH Solution as Elucidated by ESI-MS.

$$\underset{R\text{-Mn-}R}{[Mn(R\text{-phoxCOOMe})_2]^+} + \underset{S\text{-Mn-}S}{[Mn(S\text{-phoxCOOMe})_2]^+} \rightleftharpoons 2\,\underset{R\text{-Mn-}S}{[Mn(R\text{-phoxCOOMe})(S\text{-phoxCOOMe})]^+}$$

various additives. Basic additives were found to enhance epoxidation activity, while acidic additives did not result in any catalytic activity.

Another fascinating result of the studies reported in this paper is the understanding of the role of imidazole as an additive. Berkessel et al. synthesized a series of Mn−salen complexes with tethered *N*-Meim substituents.[54] The unsubstituted Mn−salen complex showed no catalytic conversion of olefins, while the complex containing the tethered imidazole showed almost complete conversions of olefins using dihydrogen peroxide as the oxidant. In the $[Mn(phox)_3]$-catalyzed epoxidations, $[Mn(phox)_2(N\text{-Meim})]^+$ has been found to be the major species present during catalysis.[22,23] Thus, coordination of the nitrogen-containing base has been assumed to be important for oxo transfer.

Complex **RS-1** has been demonstrated to be able to bind to *N*-Meim only when it is added in extremely high excess, whereas **R-1** will bind *N*-Meim when it is added in smaller amounts (only 10 equiv). It seems that in the epoxidation experiments (with 10 equiv of additive) complex **R-1** is seriously hampered by additive coordination, whereas the *meso* complex, **RS-1**, is not, which may explain the higher catalytic activity of **RS-1**.

In case of **R-1**, it appears that upon addition of *N*-Meim, one of the axial sites is blocked by *N*-Meim, and the alkene will have to approach from the remaining axial site. Hence, as a result of the steric hindrance of the ester groups, the access of the olefin to the metal center is restricted, and therefore, the lower activity can be explained. In the case of **RS-1**, the binding of *N*-Meim is not observed in catalytic conditions, and both axial sites are therefore more readily accessible for alkene approach; however, catalytic activity is not observed if no base is present in the solution. Thus, the major role of the base would be to deprotonate the dihydrogen peroxide molecule.

The oxidation of styrene by the present complexes results in the formation of phenyl acetaldehyde as the side product. Formation of phenyl acetaldehyde could result from incomplete ring formation of the epoxide followed by proton migration. The formation of phenyl acetaldehyde suggests the involvement of a Mn^V−oxo species in the catalytic cycle, while the formation of benzaldehyde suggests the attack of dioxygen to a radical intermediate followed by scission of the olefinic linkage.[55] In the oxidation of styrene using $[Mn(phox)_3]$, benzaldehyde is the main side product.[23] Thus, the present catalytic system with a substituent on the oxazoline ring shows a marked difference with that of the parent $[Mn(phox)_3]$ catalyst.

Another interesting difference is noted in the epoxidation of 1-octene. Although $[Mn(phox)_3]$ is an efficient catalyst for the epoxidation of styrene (>100 turnovers) it has been reported to have only 15 turnovers in the epoxidation of 1-octene.[52] A higher reactivity for 1-octene by the present compounds, compared to that of $[Mn(phox)_3]$, is expected because the presence of electron-withdrawing substituents is known to result in a higher number of epoxide turnovers for this substrate.[9] However, for other alkenes, the complexes show lower turnover numbers, compared to that of the previously studied $[Mn(R\text{-phox})_3]$ catalysts,[22,23] which could be the result of the increased steric bulk on the axial sites.

The manganese complexes of the phoxCOOH ligand were originally designed based on the work by Katsuki et al.,[14] who reported high asymmetric induction (>99% ee) and high turnovers in the epoxidation of 2,2-dimethylchromene derivatives using a Mn−salen complex containing a conformationally fixed carboxylate group on the ethylenediamine moiety. In general, for any catalytic activity to be observed, at least one or two axial sites have to be free for the formation of the Mn−oxo or Mn−oxetane species. In the present catalytic system (**R-4** and **RS-5**), the two carboxylate groups can block both axial sites, which would explain the lower turnover numbers (<10) relative to those of **R-1**, **R-2**, **RS-1**, and **RS-3**.

(54) Berkessel, A.; Frauenkron, M.; Schwenkreis, T.; Steinmetz, A.; Baum, G.; Fenske, D. *J. Mol. Catal. A* **1996**, *113*, 321−342.

(55) Samsel, E. G.; Srinivasan, K.; Kochi, J. K. *J. Am. Chem. Soc.* **1985**, *107*, 7606−7617.

Concluding Remarks

The manganese complexes of the racemic and enantiopure ligands HphoxCOOMe and HphoxCOOH exhibit interesting structural preferences because of the chirality on the ligands in solid state and in solution. Reaction of the *R*-phoxCOOMe ligand with a Mn(II) salt results in the formation of a Mn(III) complex in which the two ligands are bound *trans* to the metal center and the ester groups on both ligands point toward one of the axial sites on manganese (**R-1** and **R-2**). Reaction of the *RS*-phoxCOOMe ligand with a Mn(II) salt results in the formation of an Mn(III) complex in which each manganese ion is bound to two ligands that have same chirality, as observed from the solid-state structure of the **RS-1** complex. Reaction of the *R*-HphoxCOOH ligand with a Mn(II) salt results in the formation of complex **R-4** in which the ligands are bound tridentately in a *fac*-cct manner to the metal center, while a reaction of the racemic *RS*-HphoxCOOH ligand with a Mn(II) salt leads to formation of complex **RS-5** in which the two ligands are bound didentately with like atoms *trans* to the metal center. Electrochemical studies on the complexes revealed that the Mn(III)/Mn(II) reduction is quasi-reversible for all complexes and that the Mn(III)/Mn(IV) oxidation is electrochemically irreversible. Complexes **R-1**, **R-2**, **RS-1**, **RS-3**, and **RS-5** have been characterized using paramagnetic ^{1}H NMR; a tentative assignment of the observed signals was achieved using inversion-recovery pulse sequence experiments and by comparison to the previously reported [Mn(*R*-phox)$_2$] complexes.

Complexes **R-1**, **R-2**, **RS-1**, and **RS-3** show moderate epoxidation activity, with complexes **RS-1** and **RS-3** showing highest activity. A pronounced base effect of the additives was observed: the use of basic additives with p*K*'s higher than 6 resulted in an enhancement of catalytic activity, while use of acidic additives did not result in any activity.

Although no major structural differences are observed in solid-state for complexes **R-1** and **RS-1**, the solution structures have been found to be considerably different. ESI-MS studies have shown that complex **RS-1** exchanges the enantiomeric ligands in solution and changes into a *meso* structure in which two ligands of opposite chirality are bound to one metal center. Because of this ligand exchange, added *N*-Meim cannot easily coordinate to the metal as both axial sites are blocked by the ester group on each ligand. However, as complex **RS-1** shows significantly higher catalytic epoxidation activity than **R-1**, our studies indicate that imidazole binding is not necessary for good activity, in contrast with proposals in the literature. In fact, the results in this work support the increasingly popular hypothesis that "basicity is sufficient property for catalytic activity"[17] which seems to apply not only to bases such as carboxylate or carbonate salts but also to substituted imidazoles.

Acknowledgment. This work has been carried out within the framework of the Council for Chemical Sciences of The Netherlands Foundation for Scientific Research (CW-NWO) through a grant from the special program "Aspasia". X-ray crystallographic work was supported (A.L.S.) by the Council for the Chemical Sciences of The Netherlands Organization for Scientific research (CW-NWO). We would like to thank Prof. Dr. Jan Reedijk for stimulating discussions. Dr. I. W. C. E. Arends, Mr. Pedro Pereiro (Delft University of Technology) and Dr. Luke van Langen (Clea Technologies) for their help on asymmetric epoxidations and the use of chiral GC. We are grateful to Dr. F. Lefeber and Dr. C. E. Erkelens for their help on NMR studies and to Mr. J. A. P. P. van Dijk and Mrs. J. A. Erkelens-Duijndam for their help on ESI-MS and LC-MS studies.

Supporting Information Available: Tables of hydrogen bonding interactions, electrochemical data, the inversion-recovery pulse sequence for the complex **RS-5**, the ESI-MS figures, and further details in CIF format on the crystal structures of complexes **R-1**, **RS-1**, **R-2**, **R-4**, and **RS-5**, including atomic coordinates, displacement parameters, bond lengths, and bond angles. This material is available free of charge via the Internet at http://pubs.acs.org.

IC051223Z